SCIENCE CHINA
Technological Sciences

Special Topic: Superlubricity Science and Technology
•Article•

https://doi.org/10.1007/s11431-024-2719-y

Study on the tribological properties of metal rolling bearing under lubrication with diketone lubricants

DU ShaoNan[1], ZHANG ChenHui[1*] & LUO Zhi[2]

[1] *State Key Laboratory of Tribology in Advanced Equipment, Tsinghua University, Beijing 100084, China;*
[2] *Beijing National Laboratory of Molecular Sciences, CAS Key Laboratory of Engineering Plastics, Institute of Chemistry, Chinese Academy of Sciences, Beijing 100190, China*

Received March 3, 2024; accepted June 13, 2024; published online June 25, 2024

In this article, 1-(4-ethylphenyl)-nonane-1,3-dione (0206) was prepared by Claisen condensation. By mixing 0206, chelate, and base oil in a ratio of 3.2:4.8:2, a diketone lubricant (PAO=14 (20%)) that can achieve superlubricity was prepared and applied to bearing lubrication experiments. The experimental results show that when the bearing was lubricated by base oil, the friction coefficient (COF) and temperature rise decreased with the decrease of the viscosity of PAO. When PAO=14 (20%) was used as the lubricant, the COF of the bearing was the lowest (0.001), and the wear morphology was comparable to that of the bearing lubricated with commercial lubricant. Compared with the base oil with the same viscosity, it is found that the COF and temperature rise of the bearing lubricated by PAO=14 (20%) were lower under any experimental conditions. And when the amount of lubricant added was 10 μL, the COF of the bearing lubricated by PAO=14 (20%) reached a very low value (0.0004). Bearing ball surface analysis identified the formation of diketone adsorption films. Combined with the previous PAO=14 (20%) superlubricity mechanism, it was considered that the occurrence of tribochemical reaction and the bearing effect of chelates were the main reasons for the existence of ultra-low friction coefficient and low wear. In addition, when there were polar molecules in the lubricant, they were adsorbed on the metal surface through tribochemical reactions, resulting in many irregular pits on the surface.

superlubricity, diketone, chelate, tribochemical recations, bearing lubrication

Citation: Du S N, Zhang C H, Luo Z. Study on the tribological properties of metal rolling bearing under lubrication with diketone lubricants. Sci China Tech Sci, 2024, 67, https://doi.org/10.1007/s11431-024-2719-y

1 Introduction

The development of industry is closely related to rotating machinery, and bearing is the most important part of rotating machinery [1,2]. As one of the core basic components in the field of mechanical manufacturing and equipment technology, rolling bearings play an important role in carrying and transmitting power [3,4]. Rolling bearings have the advantages of easy starting, low friction coefficient (COF), and convenient replacement, so they are widely used in automobile manufacturing, precision instruments, aerospace, and other fields [5,6]. The rolling elements of the bearing are in point contact with the inner and outer raceways. The contact area is small and the contact pressure is high. Therefore, the bearing is prone to heat generation and an increase in COF during operation. With the development of aerospace and precision instruments, higher requirements are placed on the COF and temperature rise of bearings [7–10]. Improving the life of bearing components is closely related to the use of lubricant [11]. The use of higher-quality lubricants allows equipment with bearings to operate at higher loads and speeds without catastrophic consequences for the friction unit [12–14]. Wu et al. [15] showed that when adding 1 wt.% hexagonal boron nitride (hBN) and 5 wt% $CaCO_3$ nano-

*Corresponding author (email: chzhang@tsinghua.edu.cn)

particles to polyurea grease, it can not only reduce the COF of the bearing by isolation, protection, and nano-abrasive action, but also improve the vibration suppression performance. Dokshanin et al. [16] found that compared with ordinary grease, the addition of 1 wt.% ultrafine diamond-graphite powder can reduce the wear loss of the lubricated bearing by 1.6–1.8 times, the friction torque by 23%–25%, and the temperature of the bearing assembly by 16%–20%. Lineira del Rio et al. [17] found that the addition of 2 wt.% ionic liquid and 0.1 wt.% h-BN or graphene nanosheets (GnP) to triisotridecyltrimellitate (TTM) base oil reduced the COF of the bearing by increasing the oil film thickness of the lubricant and isolating the contact of the friction pair under boundary lubrication.

The study of superlubricity began in the 1980s. Hirano et al. [18] theoretically calculated the phenomenon that the two crystal planes moved in a specific direction and the friction force disappeared. In the actual experimental state, it was usually considered that the ultra-low friction state with the sliding COF lower than 0.01 was superlubricity [19]. According to the type of lubricant used in the realization of superlubricity, it can be divided into water-based superlubricity and oil-based superlubricity [20]. At present, the realization of oil-based superlubricity based on metal friction pairs usually depends on the use of lubricants that can react with friction pairs [21]. Zeng and Dong [22] found that the Nitinol 60 alloy/steel friction pair can achieve superlubricity under castor oil lubrication under boundary lubrication conditions. Ge et al. [23] found that steel/steel friction pairs lubricated with polyethylene glycol aqueous solution (PEG (aq)) can form a composite adsorption layer, which helped the friction pairs subsequently lubricated with polyalkylene glycol (PAG, polar molecule) or poly-α-olefin (PAO, nonpolar molecule) to achieve superlubricity.

In addition to selecting commercial lubricants, some scholars have studied oil-based superlubricity by preparing lubricants with specific molecular structures, the most representative of which is 1,3-diketone. The 1,3-diketone molecule has two tautomeric forms, the keto form and the enol form, and can form an octahedral chelate with metallic iron [24]. Amann and Kailer [25] found that metal friction pairs lubricated by liquid crystal fluid can exhibit extremely low COF after a certain running-in period. The contact pressure of the friction pair dropped from the initial 130 MPa to 10 MPa, making the lubricated friction pair in an elasto-hydrodynamic state. Subsequently, the author further studied and found that the friction pair lubricated by this lubricant can only achieve superlubricity when the contact pressure is very low [26]. Our team also carried out research on 1,3-diketone oil-based superlubricity. The prepared diketone molecules were 1-(4-ethylphenyl)-butane-1,3-dione (0201) and 1-(4-ethylphenyl)-nonane-1,3-dione (0206). The experiment found that the contact pressures of the two when achieving superlubricity were 19.08 and 24.70 MPa, respectively [27–29]. The mechanism of the two diketones to achieve superlubricity can be attributed to the following three points. First, the tribochemical reaction between the 1,3-diketone molecule and the metal friction pair formed an adsorption layer. Second, during the running-in process, the material of the friction pair was consumed to reduce the pressure in the contact area. Finally, the diketone molecules were oriented in the shear direction, which reduced the shear viscosity of the lubricant. Subsequently, we found that the addition of 60% of the chelate to 1,3-diketone (0206-Fe (60%)) can effectively increase the pressure of the contact area when the superlubricity is achieved [28]. In order to further evaluate the superlubricity of diketones and their chelates added to the base oil, we designed tribological experiments of diketones, chelates, and base oils with different viscosities at different mixing ratios. The experimental results showed that the lubricant prepared by mixing 0206-Fe (60%) with the base oil of the same viscosity at 8:2 has the best tribological properties [30].

This article mainly evaluates whether diketone lubricant can exert its superlubricity properties when used in bearings. This was also the first application research of diketone lubricants in the engineering field. In order to study the influence of experimental conditions on the tribological properties of bearings, experiments under different loads, rotational speeds, and lubricant additions were carried out. This study focuses on the COF, temperature rise, surface morphology of the bearing, and whether an adsorption film is formed on the surface of the friction pair. Finally, the results of this study show that the use of diketone lubrication can reduce the COF of the bearing by an order of magnitude compared with base oil and commercial lubricating oil. This study provides a reference for the application of oil-based superlubricity.

2 Materials and method

2.1 Preparation of diketone lubricant

The previous research results showed that the mixed lubricant prepared by mixing 1-(4-ethylphenyl)-nonane-1,3-dione (0206), chelate, and PAO lubricant with viscosity of 14 mPa·s (PAO=14) in an appropriate proportion showed excellent tribological properties [30]. Based on the previous research results, the mixed lubricant was prepared and named PAO=14 (20%). The specific preparation process was as follows. First, 0206 was prepared by the improved Claisen condensation method, as seen in Figure 1(a) [28]. Subsequently, 0206 was reacted with anhydrous ferric chloride to prepare a chelate (0206-Fe) of diketone and iron, which had an octahedral structure (seen in Figure 1(b)) [31]. PAO2 and PAO4 were mixed in a ratio of 4.5:5.5 to obtain PAO with a

viscosity of 14 mPa·s, named PAO=14. Finally, the above obtained 0206, 0206-Fe, and PAO=14 were mixed at a ratio of 32%, 48%, and 20%, respectively.

2.2 Bearing lubrication experiment

The friction test was carried out on a self-made high-speed bearing friction tester (HS-BFT12000). The testing machine was purchased from Lanzhou Huahui Instrument Technology Co., Ltd. Figure 2 shows the main part of the test machine, the cooling water circulation machine used to reduce the heating phenomenon of the motor and the supporting bearing during the test, and the control host used to control the experiment and collect data. The high-speed bearing friction tester used the principle of equal coaxial torque to obtain the torque signal of a pair of bearings and the temperature signal of the infrared thermometer through the sensor during the test. The above signals were amplified and inputted into the computer to obtain the bearing COF curve and temperature curve through A/D conversion and operation. The measurement ranges of the load sensor and the torque sensor were 0–300 N and 0.05–200 mN·m, respectively. The experimental speed range and temperature measurement range were 0–12000 r/min (rpm) and 0°C–150°C, respectively. In addition, special tools and standard weights were used to calibrate the axial loading sensor and torque sensor of the test machine before the start of the experiment to ensure the accuracy of the test results.

The bearing model used in the subsequent experiment was B7004C/P4, which was purchased from Luoyang Bearing Research Institute Co., Ltd. Table 1 shows the specific parameters of the angular contact ball bearings used. Figure 3

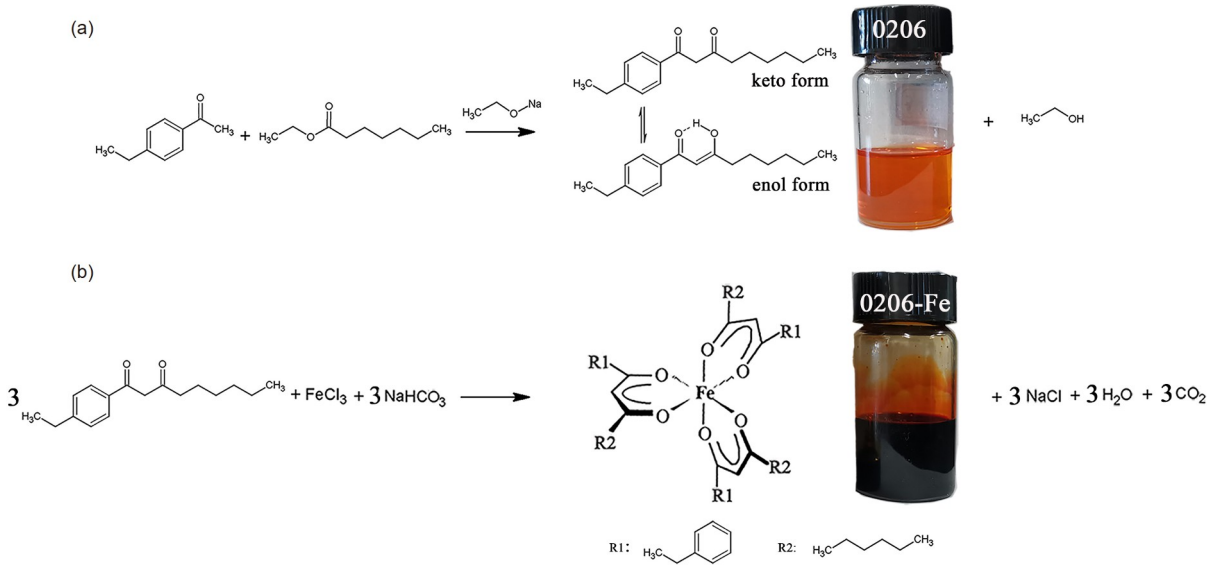

Figure 1 (Color online) Preparation process and physical diagram of (a) diketone and (b) chelate.

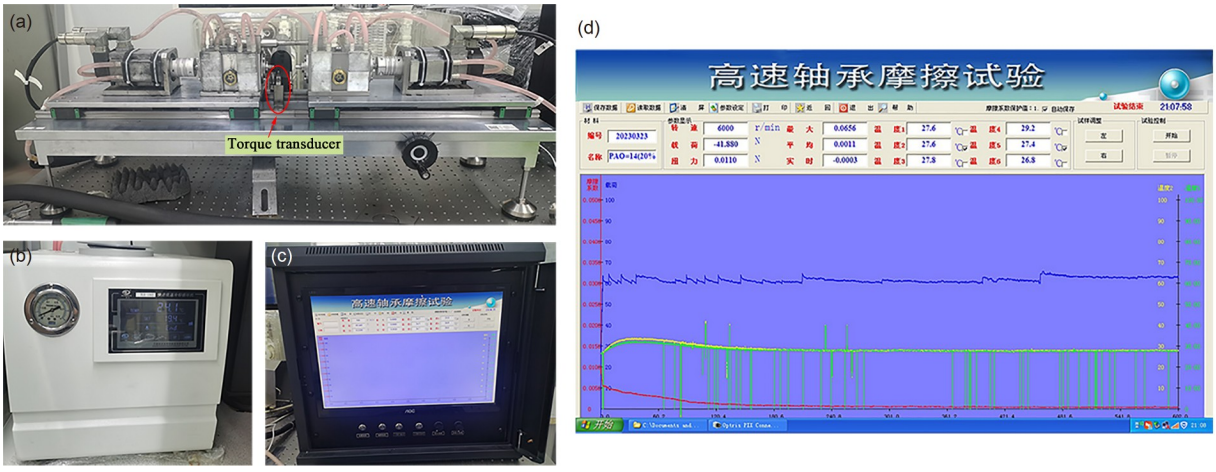

Figure 2 (Color online) Physical picture of the high-speed bearing testing machine. (a) Main part; (b) low-temperature cooling circulation device; (c) control host; (d) data collection interface during experiment.

Table 1 Angular contact ball bearing parameters used in experiments

Project	Parameter
Bearing type	B7004C
Accuracy grade	P4
Channel roughness	0.04 μm
Ball surface roughness	0.014 μm
Bearing material	GCr15
Cage material	Phenolic gum wood
Contact angle	15°
Groove curvature (f_e, f_i)	f_e=0.54, f_i=0.57
Ball diameter	Φ=5 mm
Number of balls	13

shows the physical diagram of the bearing and the assembly form of the bearing during the experiment. Before the start of the experiment, petroleum ether and anhydrous ethanol needed to be used to clean the bearing by ultrasonic method. Then, 20 μL lubricant was added between the ball and raceway of each bearing using a microsyringe. Subsequently, two bearings were installed in the fixture in the form of a back-to-back in preparation for subsequent tribological experiments. In the experiment, only the axial load was applied to the sample. The experimental time of each group of samples was 40 h, which was completed in 4 times. Each group of experimental bearings needed to be taken out and cleaned every 10 h, and then 20 μL lubricant was added to each bearing to continue the tests.

2.3 Surface characterization

The viscosity of the lubricants used in the experiment was tested using a rotadtional rheometer (MCR302, Anton P, Austria). The cross-sectional profiles of the inner and outer raceways of bearings were tested using a 3D white light interferometer (ZYGO NexView). The morphology of the ball, inner and outer raceways of the bearings was characterized using a scanning electron microscope (SEM, FEI, Quanta 200 FEG). The chemical composition of the adsorption film on the ball surface was analyzed by X-ray photoelectron spectroscopy (XPS, Ulvac-Phi lnc. PHI Quantera II, Al Kα radiation). Before starting the analysis, the surface was sputtered with argon ions at 500 V to remove hydrocarbon contaminants adsorbed from the air. The binding energy value of C 1s is 284.6 eV and was used to calibrate the binding energy.

3 Results and discussion

3.1 Tribological behavior of bearings under different lubrication conditions

Firstly, seven kinds of lubricants, 4129A, PAO10, PAO8, PAO6, PAO=14, PAO2, and PAO=14 (20%) were selected to study the tribological properties of bearings under their lubrication. 4129A was a commercial precision bearing lubricant. PAO10, PAO8, PAO6, PAO=14, and PAO2 were poly-α-olefin lubricants with different viscosities. PAO=14 (20%) was a lubricant containing diketone and chelate. The viscosity data of the above seven lubricants at 25°C are shown in Table 2. The main parameters of the bearing experiment carried out in this section were: axial loading of 60 N, rotation speed of 6000 rpm, and the amount of lubricant added to each bearing was 20 μL. The effects of different viscosities and types of lubricants on the tribological experimental results of bearings were mainly concerned.

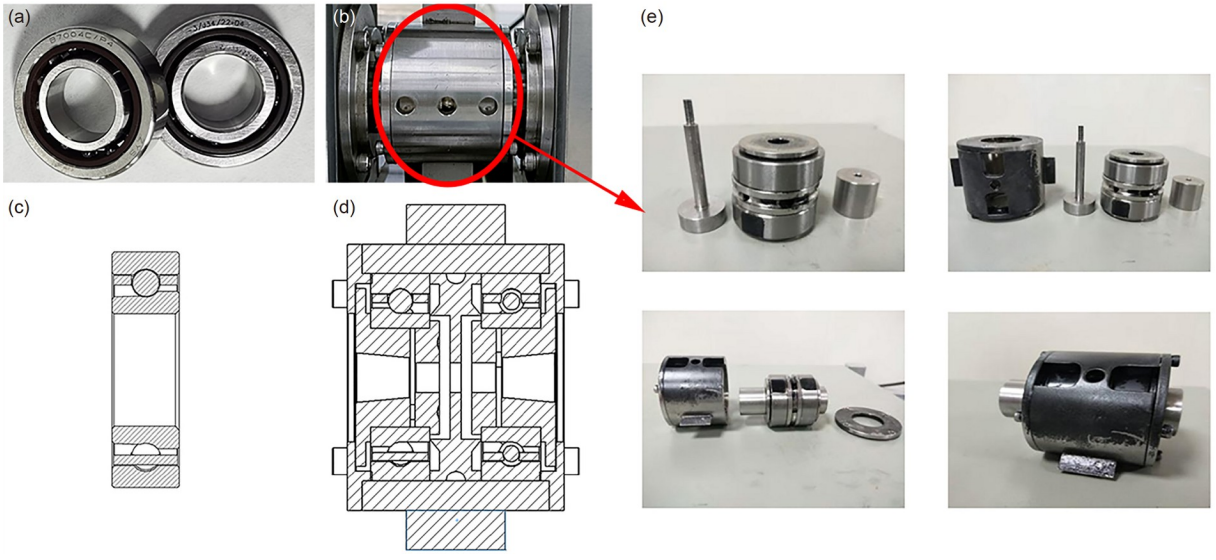

Figure 3 (Color online) (a) Physical drawings and (c) cross-sections of angular contact ball bearings; (b) physical drawings and (d) cross-sections of bearing assembly; (e) the process of bearing installation.

Table 2 Viscosity of lubricating oils used in bearing lubrication experiments

Lubricants	Viscosity (mPa·s)
4129A	106.3
PAO10	114.2
PAO8	80.5
PAO6	46.4
PAO=14	14.1
PAO2	5.8
PAO=14 (20%)	14.0

Figure 4 shows the COF curves and temperature rise curves of the bearing when using different lubricants. The experiment of each sample for 40 h was completed four times. After each experiment, the bearing needed to be cleaned and the lubricating oil needed to be added again. Therefore, there was a running-in stage in each experiment, which also explained the discontinuity of the curves in Figure 4(a) and (b). According to the infrared temperature measurement data, the initial temperature of the outer ring of the bearing at the beginning of the experiment was 26°C. Therefore, the actual measured outer ring temperature was subtracted from the initial temperature to obtain the temperature rise (ΔTemperature) curve of the outer ring of the bearing during the experiment, as shown in Figure 4(b). Observing the COF curves of bearings lubricated by PAO10, PAO8, PAO6, PAO=14, and PAO2 in Figure 4(a), it can be found that the COF decreased with the decrease of the viscosity of lubricants. This can be explained by reducing the viscous friction of the lubricating oil film formed between the rolling element and the inner and outer raceways in the bearing. In Figure 4(b), it can be found that the temperature rise of the bearing also decreased with the decrease of the viscosity of the lubricant. In addition, by observing the COF curves of bearings lubricated with the above five different viscosity base oils, it can be found that the COF curves of bearings lubricated with PAO10 and PAO8 showed a significant downward trend during the experiment. The downward trend of the COF curve of the bearing lubricated by PAO6 was obviously reduced. The COF curves of the bearings lubricated by PAO=14 and PAO2 were relatively stable after the running-in period. This is because the greater the viscosity of the lubricant, the greater the proportion of viscous friction in the bearing friction torque. Considering that the lubricant was continuously consumed by contact transfer and splashing during the experiment, the proportion of viscous friction was decreased. Friction was the main cause of bearing heating, and the decrease of COF also led to the decrease of bearing temperature rise. For bearings lubricated with low viscosity lubricants (PAO=14 and PAO2), the proportion of viscous friction in the friction torque was

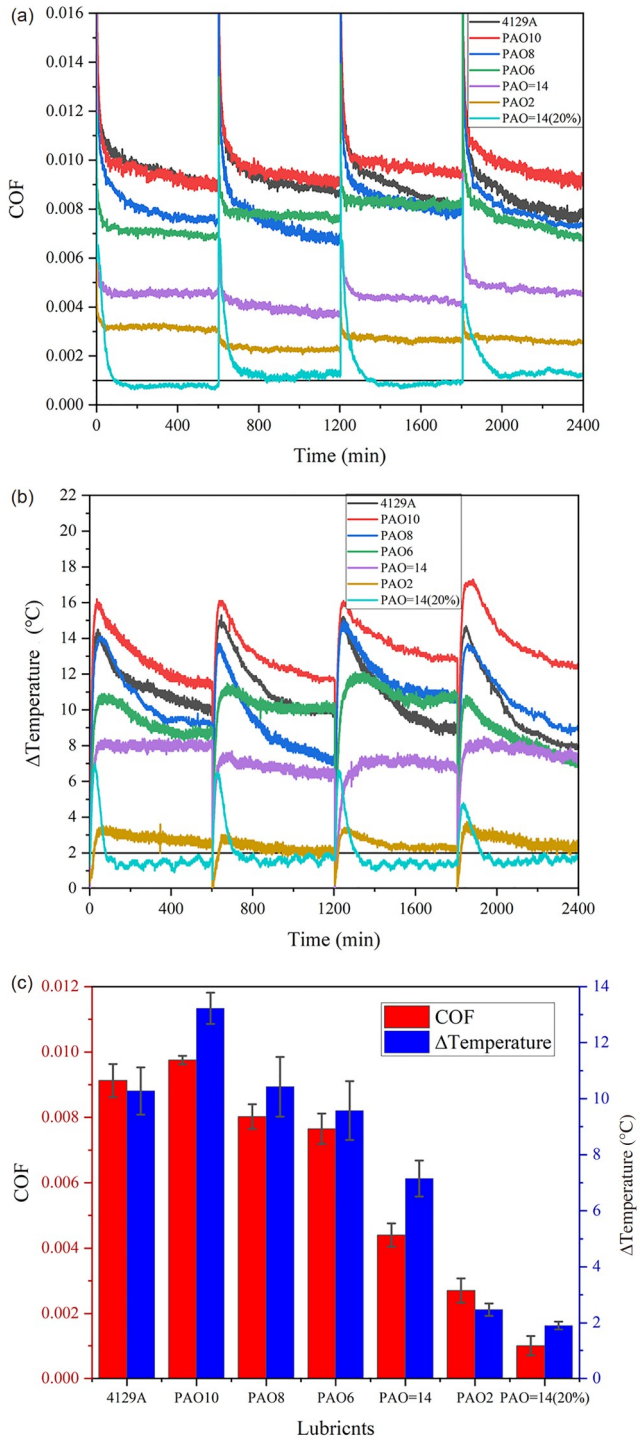

Figure 4 (a) COF, (b) temperature rise, and (c) average COF and temperature rise of bearings lubricated by seven different lubricants for 40 h.

low. The lubricant was more easily dispersed in the bearing and the lubrication state was more stable. Therefore, the COF of the bearings lubricated by them was low, and the COF changed little after the running-in period. The above theoretical explanation can also be applied to the temperature rise curves as shown in Figure 4(b).

Since both 4129A and PAO=14 (20%) lubricants con-

tained polar molecules. Therefore, the COF curve and temperature rise curve of the bearing lubricated by 4129A and PAO=14 (20%) showed different trends from the base oil. The COF of the bearing lubricated by 4129A also shows a decreasing trend with time. Especially in the third and fourth experiments, the COF curve decreased more sharply. At the end of the experiment, the COF was even comparable to that of PAO8 lubricated bearings. In addition, by observing the temperature rise curve of 4129A lubricated bearing, it was found that the temperature rise of bearing under this lubrication condition was not only lower than that of PAO10 lubricated bearing with the same viscosity grade but also lower than that of low viscosity PAO8 lubricated bearing in the third and fourth experiments. The COF of the bearings lubricated by PAO=14 (20%) in the four experimental stages were 0.0007, 0.0012, 0.0008, and 0.0013, respectively, which were much lower than those of the bearings lubricated by PAO2. Comparing the COF curves of bearings lubricated with PAO=14 (20%) and base oil PAO=14 with the same viscosity, it was found that the COF of the former reached a stable state for a long time, about 150 min, while the latter was about 50 min. The COF of the bearings lubricated by two kinds of lubricants with the same viscosity is about 0.006 within 5 min at the beginning of each experiment. Subsequently, the bearings lubricated with PAO=14 (20%) rapidly reduced the COF to about 0.001 in the following 150 min. The bearings lubricated by PAO=14 reduced the COF to about 0.0045 in the following 50 min. Therefore, it can be inferred that the mechanism of the two lubricants to reduce the COF must be different. Combined with the mechanism that PAO=14 (20%) promoted the sliding friction pair to achieve superlubricity, it can be inferred that the reason why the bearing lubricated by PAO=14 (20%) can greatly and quickly reduce the COF can be attributed to the formation of the surface tribochemical adsorption film [30]. The existence of chelates in the solution improved the bearing capacity of the lubricant, which was beneficial to isolate the direct contact of the friction pair surface and reduce the COF. The extremely low COF and excellent oil film bearing capacity made the temperature rise of the bearing in the lubrication process naturally lower. Figure 4(b) shows that the stable temperature rise of the bearing lubricated by the diketone lubricants (PAO=14 (20%)) was less than 2°C in the four experimental stages.

The above results show that under the same experimental parameters, the bearings lubricated with PAO=14 (20%) showed better tribological properties than those lubricated with PAO=14. In order to study the changes of tribological properties of bearings lubricated by two lubricants with experimental parameters, and to prove that the excellent lubrication performance of PAO=14 (20%) was related to its unique superlubricity mechanism, not the influence of specific experimental parameters, the following contents will study the influence of axial load, rotational speed, and lubricant addition on the COF and temperature rise of the bearing. Figure 5(a) and (b) show the COF of the bearing lubricated by PAO=14 and PAO=14 (20%) under axial load of 60 N, lubricant addition of 20 μL, and rotation speed of 4000–10000 rpm. The experimental conditions of the experimental results as shown in Figure 5(c) and (d) were: axial load of 40–100 N, rotation speed of 6000 rpm, and lubricant addition of 20 μL. The experimental conditions in Figure 5(e) and (f) were to ensure that the axial load of the bearing was 60 N, the rotation speed was 6000 rpm, and the amount of lubricant added was 10–40 μL. Figure 6 shows the temperature rise curve of the bearing under the same experimental conditions in Figure 5.

It can be seen from Figure 5(a) and (b) that the COF curves of bearings lubricated by PAO=14 and PAO=14 (20%) showed different variation rules with the increase of rotational speed, and their COF ranges were 0.0032–0.0057 and 0.0014–0.0006, respectively. Both the COF and temperature rise of bearings lubricated by PAO=14 increased with the increase in the rotational speed. This can be explained by the following two aspects: (1) With the increase of speed, the friction speed of the rolling friction inside the bearing increased, and the number of sliding friction between the rolling element and the raceway increased, resulting in an increase in COF and an increased in heat; (2) The centrifugal force of the ball and cage of the bearing increased with the increase of the rotational speed, and the force and collision between them and the outer ring of the bearing increased, which also led to the increase of COF and temperature rise. The COF of the bearing lubricated by PAO=14 (20%) decreased first and then increased with the increase of rotational speed. This phenomenon was also reflected in the temperature rise curves of the bearing. In addition, it can be seen from Figure 5(b) that with the increase of the rotational speed, the running-in period of the bearing lubricated by PAO=14 (20%) was shortened, and the fluctuation range of the COF curve of the bearing was also small. This phenomenon can be attributed to the fact that the increase in the rotational speed was more conducive to the reaction of diketone molecules with the metal surface to form a frictional adsorption layer. The coordination with the chelate was more conducive to isolating the direct contact of the friction pair. Therefore, when the speed was less than or equal to 7000 rpm, the COF decreased with the increase of the speed, and the temperature rise also decreased. When the rotational speed of the bearing was further increased, considering the increase of the centrifugal force of the ball and the cage, the collision between the ball and the cage, the cage and the outer ring was increased, which was the main reason for the increase of the COF and the temperature rise.

It can be seen from Figure 5(c) and (d) that the COF curves of the bearings lubricated by PAO=14 and PAO=14 (20%)

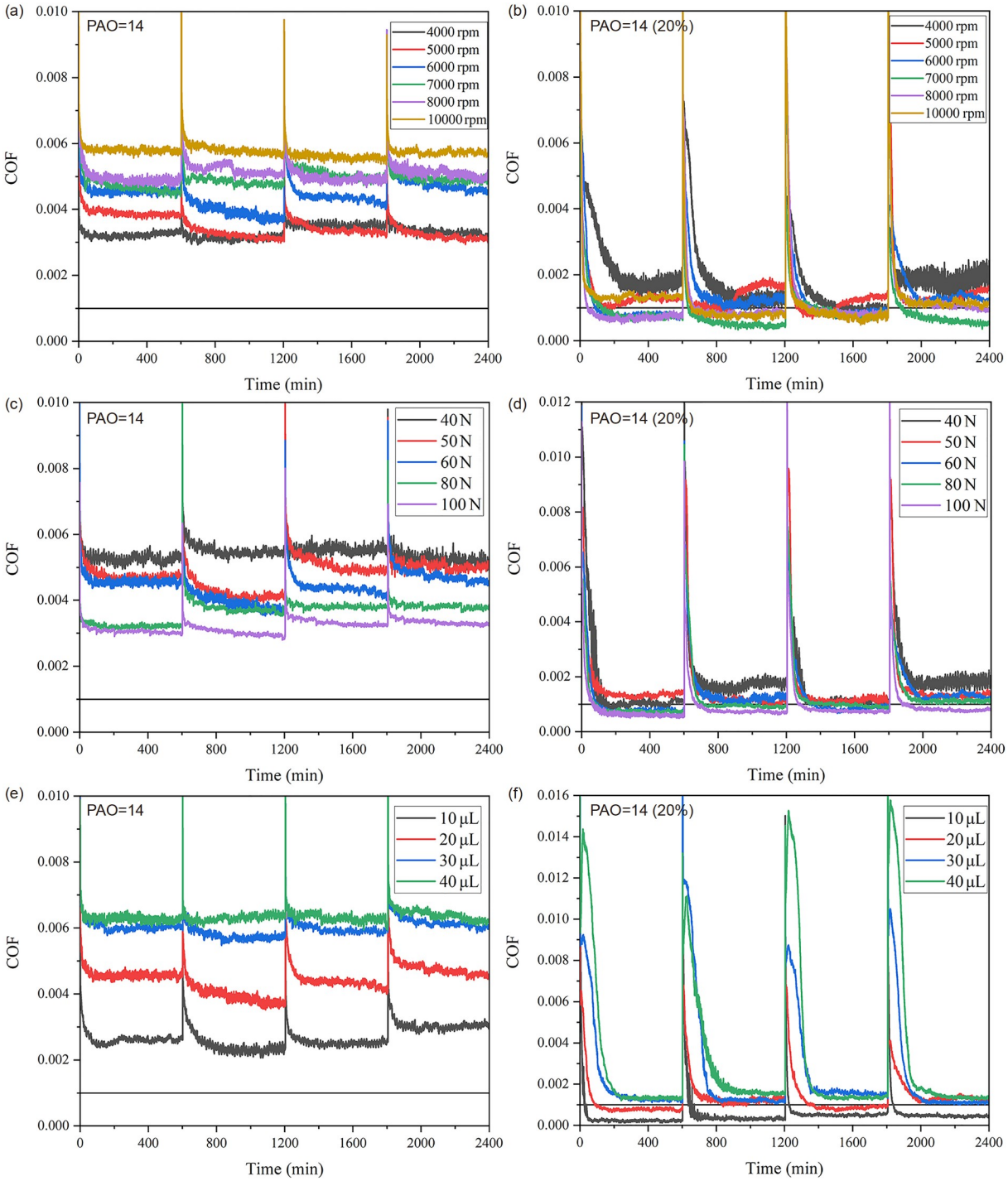

Figure 5 The COF of the bearings lubricated by PAO=14 and PAO=14 (20%) at ((a), (b)) 4000–10000 rpm, ((c), (d)) 40–100 N, and ((e), (f))10–40 μL.

showed the same variation with the increase of axial load, and their COF range from 0.0053 to 0.003 and 0.0013 to 0.0007, respectively. The COF of the bearing lubricated by PAO=14 (20%) was smaller than that of the bearing lubricated by PAO=14 under five load conditions. The running-in time required for the former to reach a stable state was longer than that of the latter. The same phenomenon was also reflected in the temperature rise curve of the bearing shown in Figure 6(c) and (d). Considering that the diketone molecules in PAO=14 (20%) needed longer time to adsorb on the surface through the tribochemical reaction, and the synergistic lubrication between the friction film and the chelate molecules was also more conducive to reducing the COF. This can explain the above experimental phenomena. According to the design principle of the bearing testing machine, the calculation formula of single bearing COF

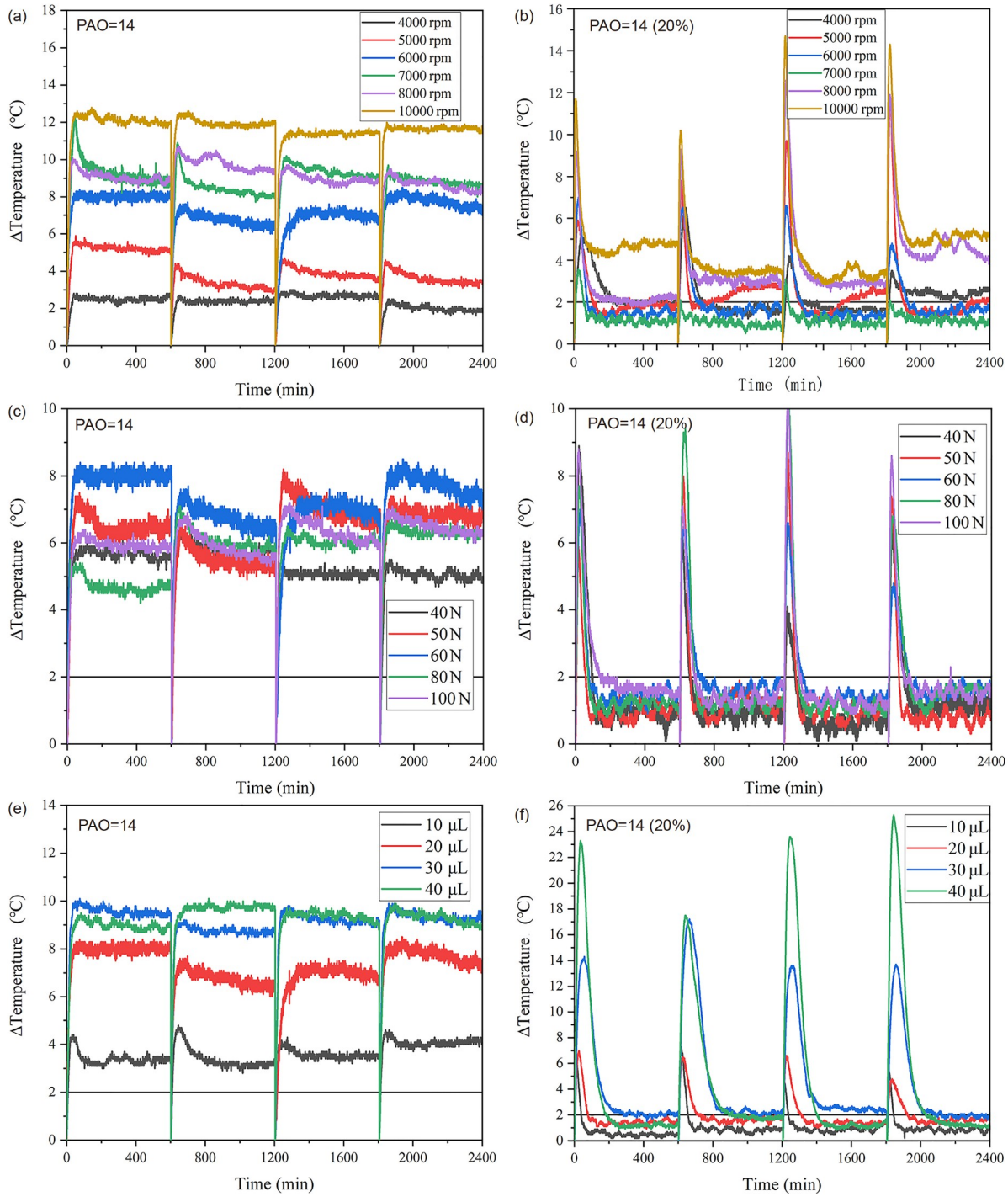

Figure 6 The temperature rise of the bearings lubricated with PAO=14 and PAO=14 (20%) under ((a), (b)) 4000–10000 rpm, ((c), (d)) 40–100 N, and ((e), (f)) 10–40 μL.

output was: $\mu=30F/(2r\cdot N)$. In the above formula, μ is the COF, F is the torsion of two bearings, N is the axial loading force, and r is the friction radius of the bearing. According to the above formula and the COF value, the average friction torque of the bearings lubricated by PAO=14 and PAO=14 (20%) with the increase of load can be calculated to be 0.0071–0.0103 N·m and 0.0017–0.0025 N·m, respectively. The friction torque of the bearing lubricated by the two lubricants increased with the increase of the load. This can be explained that the friction torque of the bearing was mainly composed of the pure rolling friction torque caused by the elastic hysteresis of the material, the friction torque caused by the differential sliding, and the friction torque caused by the spin sliding of the rolling element, and the three increased

with the increase of the load [32–34].

It can be seen from Figure 5(e) and (f) that the COF of the bearing lubricated by the two lubricants increased with the increase of the amount of lubricant added. With the increase of lubricant addition, the ACOF of bearings lubricated by PAO=14 and PAO=14 (20%) ranged from 0.0026 to 0.0063 and 0.0004 to 0.0015, respectively. When the amount of lubricant added increased from 10 μL to 20 μL, the COF of the bearing increased by 65.4% and 150%, respectively. Subsequently, as the amount of lubricant added increases, the increase in COF gradually decreases. When the amount of lubricant added increased from 30 μL to 40 μL, the increase in COF was only 6.8% and 15.4%, respectively. The increase in the amount of lubricant added will cause the movement resistance of the rolling element to increase, which was also one of the reasons for the increase in the COF. On the other hand, the change in the lubrication state caused by the increase of lubricant addition was also the main reason for the slowing down of the increasing trend of COF. It can be seen from Figure 5(f) that with the increase of the amount of lubricant added, the running-in period of the bearing became longer, indicating that it takes a longer time for the tribochemical reaction to enter a stable superlubricity state. The temperature rise curve as shown in Figure 6(e) and (f) had the same change phenomenon as the friction coefficient curve. In particular, it should be noted that the temperature rise of the bearing lubricated by PAO=14 (20%) was still controlled at about 2°C under a steady state, even if 40 μL of lubricant was added.

3.2 Surface characterization

In order to further evaluate the tribological properties of bearings lubricated by 4129A, PAO10, PAO=14, and PAO=14 (20%), the microscopic morphology of the ball, inner ring, and outer ring raceways of the above bearings was studied by SEM (seen in Figure 7) and the cross-sectional profile of the wear zone was tested by three-dimensional white light (seen in Figure 8) [35–38]. In order to make a comparative study, the contrast samples without experiments were also observed by SEM. From Figure 8, it can be seen that the wear scar depth of bearings lubricated with commercial lubricating oil (4129A) containing additives was less than that of PAO10. From the third and fourth rows of the bearing morphology photos in Figure 7, it can be found that the decrease in the viscosity of the lubricant will lead to a significant increase in the wear morphology of the ball and raceway of the bearing. The raceway of the bearing lubricated by PAO=14 showed obvious traces of abrasive wear and ploughing. It can be seen from the last row of bearing morphology photos in Figure 7 that compared with the base oil PAO=14 with the same viscosity, the wear depth of the ball and raceway of the bearing lubricated by PAO=14 (20%) was obviously shallower, and the phenomenon of abrasive wear and ploughing also disappeared. According to the previously mentioned superlubricity mechanism of diketone lubricants (PAO=14 (20%)), this phenomenon can be attributed to the formation of a diketone frictional adsorption film and the synergistic lubrication of the chelate. Another noteworthy phenomenon was that uneven micro-pits appeared on the surface of bearing balls lubricated by 4129A and PAO=14 (20%). Combining the properties of the two lubricants, this phenomenon can be initially attributed to the reaction between the polar molecules in the lubricant and the metal surface. In order to prove this conjecture, two sets of experiments were carried out to investigate the influence of the presence of polar molecules on the surface morphology of bearing balls. The experimental results are shown in Figures 8 and 9, respectively. The following will be combined with the specific experimental results to further prove the explanation of the above phenomenon.

Firstly, in order to verify the non-contingency of the above experimental results, the bearings lubricated by PAO=14 and PAO=14 (20%) under the conditions of 60 N, 6000 rpm, 10 μL and 60 N, 4000 rpm, 20 μL were selected for SEM characterization again. From Figure 8, under the same experimental parameters, the wear marks of the balls and inner ring raceways of the bearings lubricated by PAO=14 were deeper than those of the bearings lubricated by PAO=14 (20%). When the amount of lubricant added was 10 μL, it was found that the surface of the inner ring of the bearing had more obvious abrasive wear than the amount of lubricant added of 20 μL. The most important point was to observe that the ball surface of the bearing lubricated by PAO=14 (20%) still had irregular micro-pits. Comparing the ball surface morphology of the bearing lubricated by PAO=14 (20%) in Figure 7, it can be found that reducing the amount of lubricant added or reducing the bearing speed can weaken the irregular micro-pits on the ball surface. The decrease in the number of micro-pits on the surface of the bearing ball lubricated by PAO=14 (20%) at 4000 rpm can be explained by the weakening of the diketone tribo-chemical reaction. This also confirmed the experimental results of the larger COF of the bearing as shown in Figure 5(a).

The results of the two sets of experiment results as shown in Figure 10 were used to further verify that the occurrence of frictional chemical reactions during the bearing experiment resulted in the occurrence of micro-pits on the ball surface. The composition of the two lubricants used in the experiment was as follows: (1) PAO=14 (95%) was prepared by adding 5% zinc dialkyldithiophosphate (ZDDP) to PAO=14; (2) 0206-Fe (80%) was prepared by mixing 0206-Fe with PAO=14 in a ratio of 8:2. Compared with PAO=14, the COF and temperature rise of the bearings lubricated with PAO=14 (95%) were reduced by 4.9% and 10.3%, respectively, and the reduction was not obvious. However, by observing

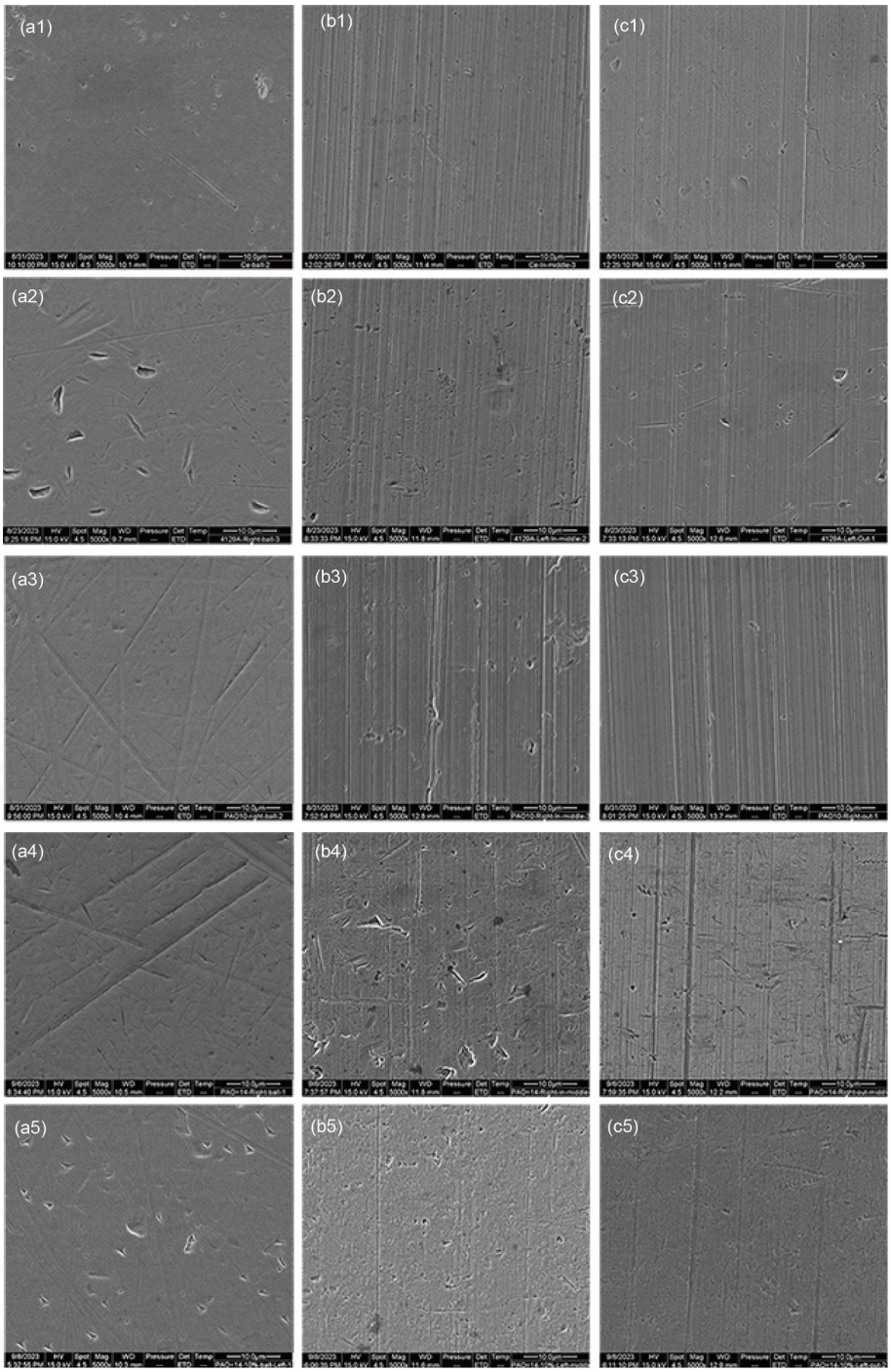

Figure 7 SEM images of (a) the balls, (b) bearing inner rings, and (c) bearing outer rings lubricated by (a2)–(c2) 4129A, (a3)–(c3) PAO10, (a4)–(c4) PAO=14, and (a5)–(c5) PAO=14 (20%) were 5000 times magnified images.

Figure 10(c)–(e), it can be found that the presence of ZDDP significantly reduced the depth of bearing wear marks and the degree of abrasive wear. In addition, it was also found that there were obvious micro-pits on the surface of the steel ball. It can be seen from Figure 10(f) that when the diketone component in the mixed lubricant was missing, the COF curve of the bearing could not be greatly reduced. In addition, it can be found from Figure 10(h)–(j) that the micro-pits on the ball surface of the bearing lubricated by 0206-Fe (80%) disappeared, while the abrasive wear and wear scar depth increased. It can be considered that the presence of diketone in the mixed lubricant adsorbed on the metal surface through the tribochemical reaction, thereby reducing the COF and alleviating the wear of the bearing. The occurrence of tribochemical reactions also led to the occurrence of irregular corrosion micro-pits on the surface of bearing balls.

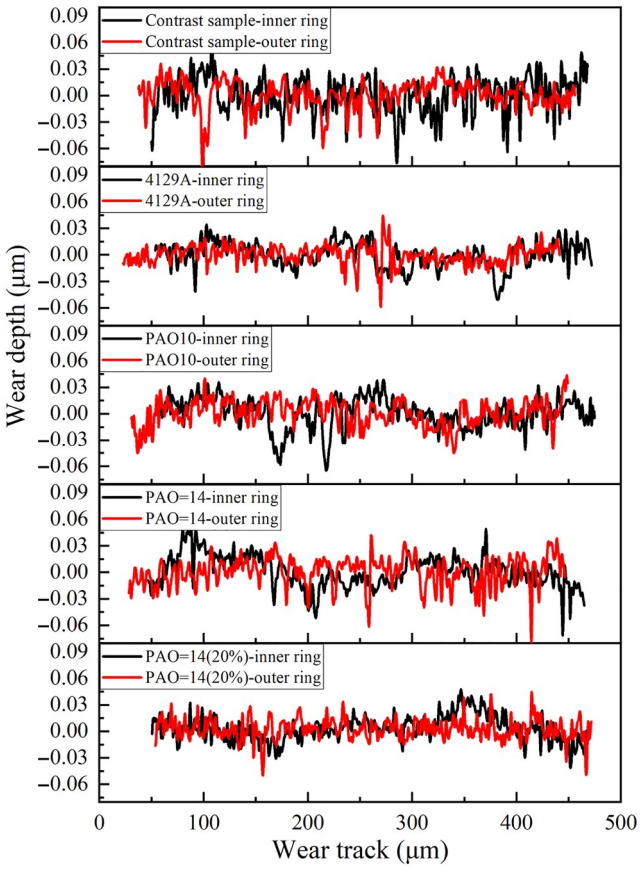

Figure 8 The cross-sectional profile of the wear zone under lubrication of 4129A, PAO10, PAO=14, and PAO=14 (20%).

Furthermore, XPS spectra were performed on the ball surfaces lubricated by PAO=14, PAO=14 (20%), and 4129A to investigate and evaluate the elements on the tribological interfaces. XPS spectrum was used to analyze the parameters of C 1s, O 1s, P 2p, and S 2p. From the molecular structures of 0206 in Figure 1(a), it can be seen that 0206 had three kinds of C atoms and two kinds of O atoms with different binding energies. In particular, C=O close to the benzene ring in the enol-type conformation had a lower binding energy than ordinary C=O due to the conjugation of the benzene ring and intramolecular hydrogen bond [28]. As shown in Figure 11, the C 1s spectrums of the steel surface lubricated by 0206 could be differentiated into four peaks due to the different chemical environments of C atoms. The binding energy of each component is shown in Table 3. These results showed that 0206 were indeed adsorbed on the surface of the metal friction pair. Observing the P 2p and S 2p spectra of the ball surface lubricated by PAO=14 (95%) proved that the ZDDP contained in the lubricant also had a tribochemical reaction with the metal surface [39]. As a commercial lubricating oil, 4129A was not clear about its specific components. However, from the C 1s, O 1s, and P 2p peak spectra of the XPS spectrum, it can be seen that it should contain organophosphorus additives and ester oils, which also indicates that polar additives can still chemically adsorb on the metal surface. It was found that only the C-C absorption peak was found in the C 1s spectrum of the friction pair surfaces lubricated by PAO=14. It showed that the physical adsorption film formed by this lubricant was easy to remove during ultrasonic cleaning. The above results also proved once again that the occurrence of tribochemical reaction was closely related to the micro-pits on the surface of steel balls.

3.3 Exploring the mechanism of superlubricity

The above experimental results show that under the same experimental parameters, the COF, temperature rise, and wear morphology of bearings lubricated by different base

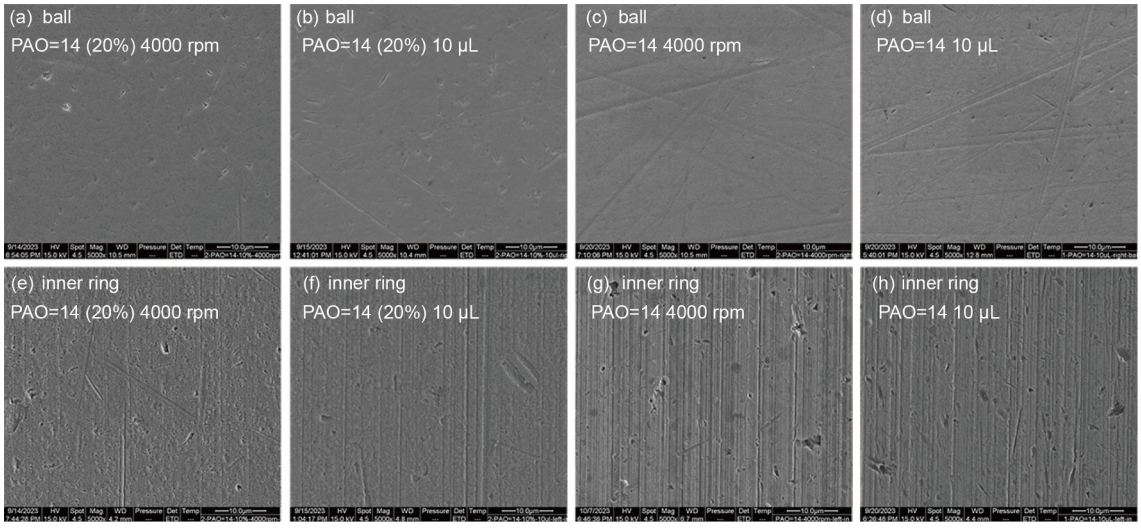

Figure 9 SEM of ((a)–(d)) the balls and ((e)–(h)) inner rings of bearings lubricated by ((c), (d), (g), and (h)) PAO=14 and ((a), (b), (e), and (f)) PAO=14 (20%) under ((b), (d), (f), and (h)) 60 N, 6000 rpm, 10 μL and ((a), (c), (e), and (g)) 60 N, 4000 rpm, 20 μL.

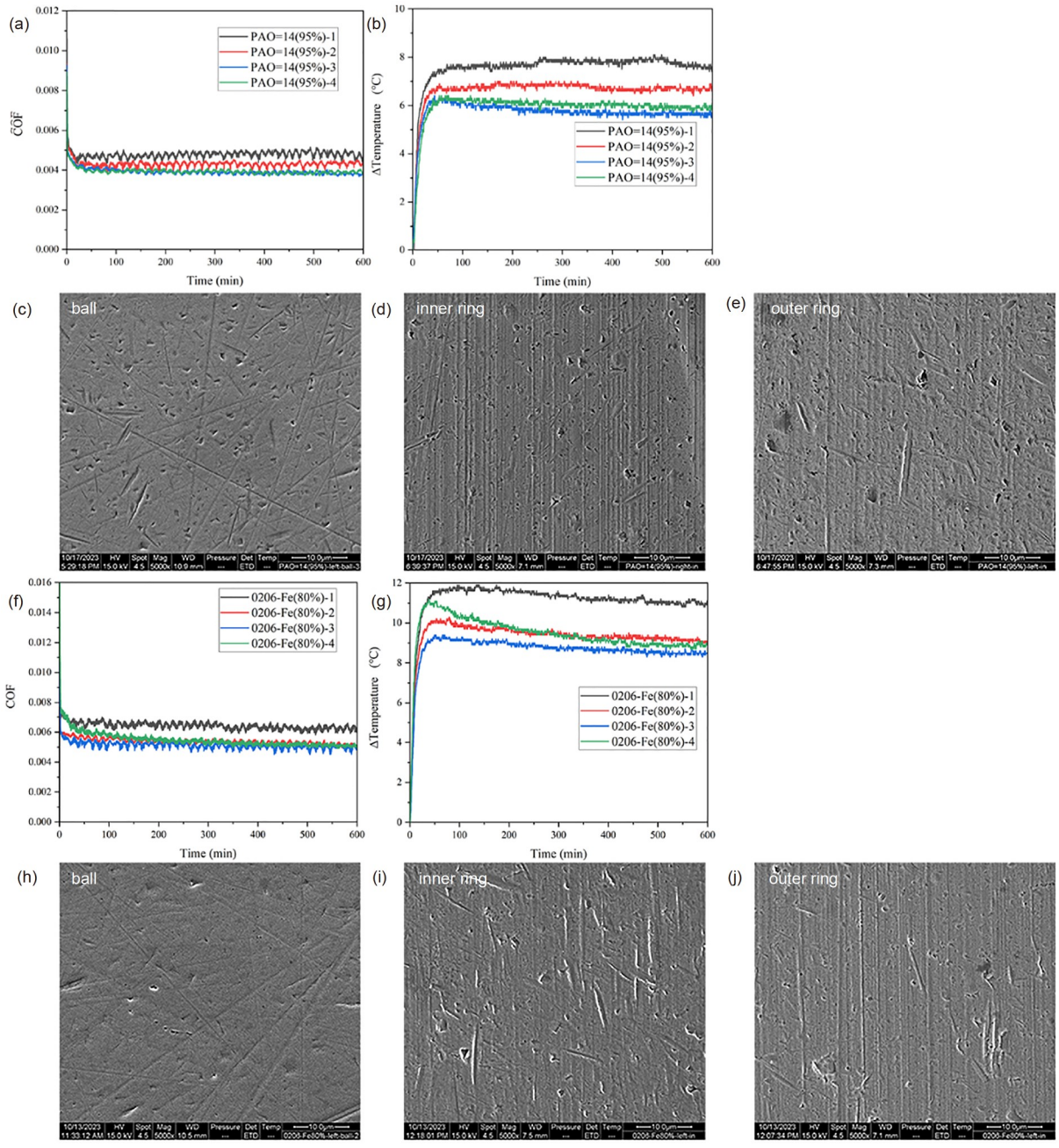

Figure 10 ((a), (f)) COF and ((b), (g)) temperature rise of bearings lubricated by 0206-Fe (80%) and PAO=14 (95%); SEM of ((h)–(j)) 0206-Fe (80%) and ((c)–(e)) PAO=14(95%).

oils were closely related to the viscosity of the lubricant. The greater the viscosity of the base oil, the higher the COF, and the higher the temperature rise, and the smaller the wear of the lubricated bearing. For the lubricant PAO=14 (20%) containing diketone and chelate, the COF and temperature rise of the friction pair lubricated by it were not only lower than that of the base oil with the same viscosity but also the wear morphology of the friction pair was even better than that of the commercial lubricant 4129A. Observing the surface morphology of bearings lubricated by different lubricants by SEM, it was found that although the wear scar depth of bearings lubricated by PAO=14 (20%) was shallow, there were more irregular micro-pits on the surface of balls. The same phenomenon also occurred on the surface of bearing balls lubricated by 4129A and lubricant containing ZDDP (PAO=14 (95%)). This indicated that the presence of polar molecules in the lubricant was adsorbed on the metal surface through the tribo-chemical reaction, resulting in the occurrence of micro-pits on the ball surface. The subsequent XPS experimental results also proved the above conclusions. Comparing the experimental results in Figures 7 and 10, it can be found that when the diketone component in PAO=14

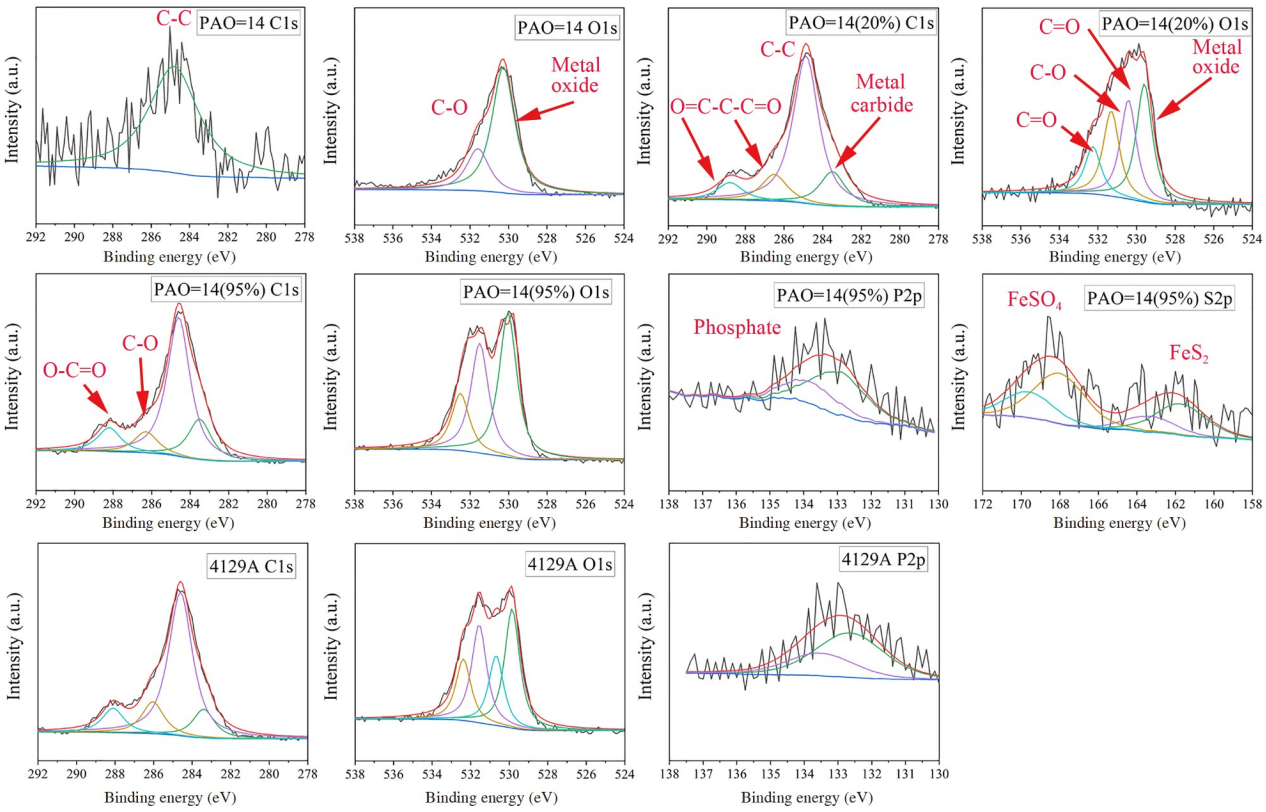

Figure 11 C 1s, O 1s, P 2p, and S 2p spectra on the surface of the balls lubricited by PAO=14, PAO=14 (20%), PAO=14 (95%), and 4129A.

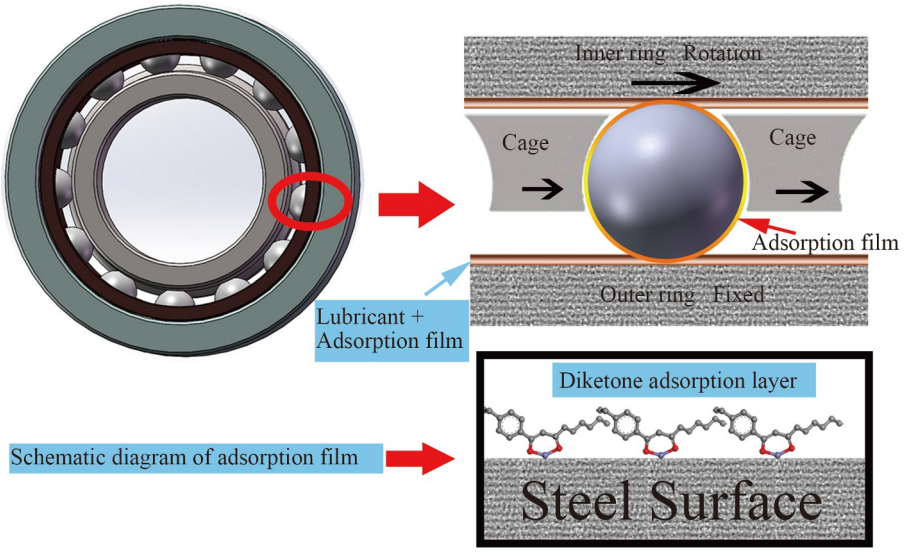

Figure 12 The lubrication mechanism diagram of PAO=14 (20%) lubricated bearing to achieve ultra-low COF (less than 0.001).

(20%) was removed, the COF and temperature rise of the lubricated bearing increased. Although there was no corrosion pit on the surface of the ball, there were obvious abrasive wear and scratch marks on the inner and outer ring raceways. Comparing the deep furrow ploughing morphology of the outer ring of the bearing lubricated by PAO=14, it was shown that the chelate contained in the base oil can effectively carry and reduce the wear of the friction pair, which was also proved in previous studies.

Based on the above experimental results and analysis, the lubrication mechanism of PAO=14 (20%) lubricated bearing to achieve ultra-low friction (less than 0.001) was proposed.

Table 3 Parameters of C 1s and O 1s components on the surface lubricated with PAO=14, PAO=14 (20%), 4129A, and PAO=14 (95%)

Binding energy (eV)		PAO=14	PAO=14 (20%)	PAO=14 (95%)	4129A
C 1s	Metal carbide	/	283.5	283.5	283.5
	C-C	284.8	284.8	284.8	284.8
	C-O	/	/	286.3	286.5
	O=C-C	/	286.5	/	/
	O=C-O	/	/	288.2	288.4
	C=O	/	288.8	/	/
O 1s	Metal oxide	530.1	530.0	530.0	530.0
	C=O (closed to benzene)	/	530.5	/	530.6
	C-O	531.5	531.4	531.5	531.5
	C=O	/	532.4	532.5	532.4
S 2p	FeS_2	/	/	161.7	/
	$FeSO_4$	/	/	168.0	/
P 2p	Phosphate	/	/	133.0	133.2

By setting up control experiments and surface XPS characterization, it can be found that the presence of diketones was conducive to the emergence of ultra-low COF and low temperature rise of bearings, and the presence of chelates was conducive to isolating the contact of friction pairs to achieve lower wear. In addition, except for the formation of tribo-chemical adsorption film on the surface, the phenomenon of micro-pits on the surface of bearing balls was also an unexpected phenomenon related to tribo-chemical reaction.

4 Conclusions

In this study, the tribological properties of bearings lubricated with different viscosities and types of lubricants were first discussed. Then, the changes of bearing COF and temperature rise with load, speed, and lubricant addition amount under the lubrication of base oil and diketone lubricant with the same viscosity were focused on. Subsequently, the surface analysis and control group experiments provide a basis for the ultra-low COF of diketone. Based on the above experiments and analysis, the following conclusions can be drawn.

(1) Under the same experimental parameters, the COF and temperature rise of the bearing decreased with the decrease of the viscosity of the base oil. However, when the bearing was lubricated with PAO=14 (20%), the COF and temperature rise of the bearing were 0.0010 and 1.8 °C, respectively, even lower than that of the bearing lubricated with the lowest viscosity base oil (PAO2).

(2) The COF of the bearing lubricated with PAO=14 (base oil) increased with the increase of load, speed, and lubricant addition. The COF of the bearing lubricated with the PAO=14 (20%) (diketone lubricant) decreased with the increase of load, decreased first and then increased with the increase of rotational speed, and increased with the increase of lubricant addition. When the amount of lubricant added was 10 μL, the bearing lubricated by PAO=14 (20%) had an extremely low COF (0.0004).

(3) When the lubricant contained polar additives, which can be adsorbed on the metal surface by tribochemical reaction during the lubrication process, micro-pits would appear on the surface of the lubricated bearing ball.

This work was supported by the National Key R&D Program of China (Grant No. 2020YFA0711003), the National Natural Science Foundation of China (Grant No. 51925506), and the National Natural Science Foundation of China Youth Science Foundation (Grant No. 52305178).

1 Dhanola A, Garg H C. Tribological challenges and advancements in wind turbine bearings: A review. Eng Fail Anal, 2020, 118: 104885
2 Wei Y, Li Y, Xu M, et al. A review of early fault diagnosis approaches and their applications in rotating machinery. Entropy, 2019, 21: 409
3 Sadabadi H, Sanati Nezhad A. Nanofluids for performance improvement of heavy machinery journal bearings: A simulation study. Nanomaterials, 2020, 10: 2120
4 Alves D S, Machado T H, Cavalca K L, et al. Characteristics of oil film nonlinearity in bearings and its effects in rotor balancing. J Sound Vib, 2019, 459: 114854
5 Xie Z L, Jiao J, Yang K, et al. Investigation on the stability and anti-eccentric load margin of a novel structure bearing lubricated by low viscosity medium. Sci China Tech Sci, 2022, 65: 1613–1633
6 Santos N D S A, Roso V R, Faria M T C. Review of engine journal bearing tribology in start-stop applications. Eng Fail Anal, 2020, 108: 104344
7 Zhang Z, Zhang H, Wang J, et al. Study on mechanics and high temperature tribological properties of porous bearing cage material. J Reinforced Plasts Compos, 2023, 07316844231201479
8 Kumar N, Satapathy R K. Bearings in aerospace, application, distress, and life: A review. J Fail Anal Preven, 2023, 23: 915–947
9 Gupta P K, Gibson H G. Real-time dynamics modeling of cryogenic ball bearings with thermal coupling. J Tribol, 2021, 143: 031201

10 Rejith R, Kesavan D, Chakravarthy P, et al. Bearings for aerospace applications. Tribol Int, 2023, 181: 108312
11 Nicholas G, Howard T, Long H, et al. Measurement of roller load, load variation, and lubrication in a wind turbine gearbox high speed shaft bearing in the field. Tribol Int, 2020, 148: 106322
12 Berman D, Erdemir A, Sumant A V. Graphene: A new emerging lubricant. Mater Today, 2014, 17: 31–42
13 Pimenov D Y, Mia M, Gupta M K, et al. Resource saving by optimization and machining environments for sustainable manufacturing: A review and future prospects. Renew Sustain Energy Rev, 2022, 166: 112660
14 Said Z, Rahman S M A, Sohail M A, et al. Nano-refrigerants and nano-lubricants in refrigeration: Synthesis, mechanisms, applications, and challenges. Appl Therm Eng, 2023, 233: 121211
15 Wu C, Xie Y, Zhao H, et al. Effects of hBN and $CaCO_3$ nanoparticles on tribological and vibration properties of polyurea grease on rolling bearing. Tribol Lett, 2022, 70: 95
16 Dokshanin S G, Tynchenko V S, Bukhtoyarov V V, et al. Investigation of the tribological properties of ultrafine diamond-graphite powder as an additive to greases. IOP Conf Ser-Mater Sci Eng, 2019, 560: 012192
17 Liñeira del Río J M, López E R, Gonçalves D E P, et al. Tribological properties of hexagonal boron nitride nanoparticles or graphene nanoplatelets blended with an ionic liquid as additives of an ester base oil. Lubrication Sci, 2021, 33: 269–278
18 Hirano M, Shinjo K, Kaneko R. Observation of superlubricity by scanning tunneling microscopy. Phys Rev Lett, 1997, 78: 14481451
19 Chen X, Li J. Superlubricity of carbon nanostructures. Carbon, 2020, 158: 1–23
20 Matta C, Joly-Pottuz L, De Barros Bouchet M I, et al. Superlubricity and tribochemistry of polyhydric alcohols. Phys Rev B, 2008, 78: 085436
21 Li J, Zhang C, Deng M, et al. Superlubricity of silicone oil achieved between two surfaces by running-in with acid solution. RSC Adv, 2015, 5: 30861–30868
22 Zeng Q, Dong G. Influence of load and sliding speed on super-low friction of Nitinol 60 alloy under castor oil lubrication. Tribol Lett, 2013, 52: 47–55
23 Ge X, Halmans T, Li J, et al. Molecular behaviors in thin film lubrication—Part three: Superlubricity attained by polar and nonpolar molecules. Friction, 2019, 7: 625–636
24 Amann T, Kailer A, Beyer-Faiß S, et al. Development of sintered bearings with minimal friction losses and maximum life time using infiltrated liquid crystalline lubricants. Tribol Int, 2016, 98: 282–291
25 Amann T, Kailer A. Ultralow friction of mesogenic fluid mixtures in tribological reciprocating systems. Tribol Lett, 2010, 37: 343–352
26 Amann T, Kailer A. Analysis of the ultralow friction behavior of a mesogenic fluid in a reciprocating contact. Wear, 2011, 271: 1701–1706
27 Li K, Zhang S, Liu D, et al. Superlubricity of 1,3-diketone based on autonomous viscosity control at various velocities. Tribol Int, 2018, 126: 127–132
28 Du S, Zhang C, Luo Z. The synergistic effect of diketone and its chelate enables macroscale superlubricity for a steel/steel contact. Tribol Int, 2022, 173: 107610
29 Zhang S, Zhang C, Li K, et al. Investigation of ultra-low friction on steel surfaces with diketone lubricants. RSC Adv, 2018, 8: 9402–9408
30 Du S, Zhang C, Luo Z. Combination of diketone and PAO to achieve macroscale oil-based superlubricity at relative high contact pressures. Friction, 2024, 12: 869–883
31 Li K, Jiang J, Amann T, et al. Evaluation of 1,3-diketone as a novel friction modifier for lubricating oils. Wear, 2020, 452-453: 203299
32 Olaru D N, Bălan M R D, Tufescu A, et al. Influence of the cage on the friction torque in low loaded thrust ball bearings operating in lubricated conditions. Tribol Int, 2017, 107: 294–305
33 Wikstrom V, Hoglund E. Starting and steady-state friction torque of grease-lubricated rolling element bearings at low temperatures-Part Ⅱ: Correlation with less-complex test methods. Tribol T, 2008, 25: 684–690
34 Houpert L. Ball bearing and tapered roller bearing torque: Analytical, numerical and experimental results. Tribol Trans, 2002, 45: 345–353
35 Sia S Y, Sarhan A A D. Morphology investigation of worn bearing surfaces using SiO_2 nanolubrication system. Int J Adv Manuf Technol, 2014, 70: 1063–1071
36 Schöfer J, Rehbein P, Stolz U, et al. Formation of tribochemical films and white layers on self-mated bearing steel surfaces in boundary lubricated sliding contact. Wear, 2001, 248: 7–15
37 Baskar S, Sriram G, Arumugam S. Tribological analysis of a hydrodynamic journal bearing under the influence of synthetic and biolubricants. Tribol Trans, 2017, 60: 428–436
38 Ren Z, Li B, Zhou Q. Rolling contact fatigue crack propagation on contact surface and subsurface in mixed mode I+II+III fracture. Wear, 2022, 506-507: 204459
39 Zhang Y, Zeng X, Wu H, et al. The tribological chemistry of a novel borate ester additive and its interaction with ZDDP using XANES and XPS. Tribol Lett, 2014, 53: 533–542